Chapter 1

Introduction

The Compact Muon Solenoid (CMS) detector is a multi-purpose apparatus due to operate at the Large Hadron Collider (LHC) at CERN. The LHC is presently being constructed in the already existing 27-km LEP tunnel in the Geneva region. It will yield head-on collisions of two proton (ion) beams of 7 TeV (2.75 TeV per nucleon) each, with a design luminosity of $10^{34}\,\mathrm{cm}^{-2}\mathrm{s}^{-1}$ ($10^{27}\,\mathrm{cm}^{-2}\mathrm{s}^{-1}$). This paper provides a description of the design and construction of the CMS detector. CMS is installed about 100 metres underground close to the French village of Cessy, between Lake Geneva and the Jura mountains.

The prime motivation of the LHC is to elucidate the nature of electroweak symmetry breaking for which the Higgs mechanism is presumed to be responsible. The experimental study of the Higgs mechanism can also shed light on the mathematical consistency of the Standard Model at energy scales above about 1 TeV. Various alternatives to the Standard Model invoke new symmetries, new forces or constituents. Furthermore, there are high hopes for discoveries that could pave the way toward a unified theory. These discoveries could take the form of supersymmetry or extra dimensions, the latter often requiring modification of gravity at the TeV scale. Hence there are many compelling reasons to investigate the TeV energy scale.

The LHC will also provide high-energy heavy-ion beams at energies over 30 times higher than at the previous accelerators, allowing us to further extend the study of QCD matter under extreme conditions of temperature, density, and parton momentum fraction (low-x).

Hadron colliders are well suited to the task of exploring new energy domains, and the region of 1 TeV constituent centre-of-mass energy can be explored if the proton energy and the luminosity are high enough. The beam energy and the design luminosity of the LHC have been chosen in order to study physics at the TeV energy scale. A wide range of physics is potentially possible with the seven-fold increase in energy and a hundred-fold increase in integrated luminosity over the previous hadron collider experiments. These conditions also require a very careful design of the detectors.

The total proton-proton cross-section at $\sqrt{s} = 14\,\mathrm{TeV}$ is expected to be roughly 100 mb. At design luminosity the general-purpose detectors will therefore observe an event rate of approximately 10^9 inelastic events/s. This leads to a number of formidable experimental challenges. The online event selection process (*trigger*) must reduce the huge rate to about 100 events/s for storage and subsequent analysis. The short time between bunch crossings, 25 ns, has major implications for the design of the read-out and trigger systems.

At the design luminosity, a mean of about 20 inelastic collisions will be superimposed on the event of interest. This implies that around 1000 charged particles will emerge from the interaction region every 25 ns. The products of an interaction under study may be confused with those from other interactions in the same bunch crossing. This problem clearly becomes more severe when the response time of a detector element and its electronic signal is longer than 25 ns. The effect of this pile-up can be reduced by using high-granularity detectors with good time resolution, resulting in low occupancy. This requires a large number of detector channels. The resulting millions of detector electronic channels require very good synchronization.

The large flux of particles coming from the interaction region leads to high radiation levels, requiring radiation-hard detectors and front-end electronics.

The detector requirements for CMS to meet the goals of the LHC physics programme can be summarised as follows:

- Good muon identification and momentum resolution over a wide range of momenta and angles, good dimuon mass resolution ($\approx 1\%$ at 100 GeV), and the ability to determine unambiguously the charge of muons with $p < 1$ TeV;
- Good charged-particle momentum resolution and reconstruction efficiency in the inner tracker. Efficient triggering and offline tagging of τ's and b-jets, requiring pixel detectors close to the interaction region;
- Good electromagnetic energy resolution, good diphoton and dielectron mass resolution ($\approx 1\%$ at 100 GeV), wide geometric coverage, π^0 rejection, and efficient photon and lepton isolation at high luminosities;
- Good missing-transverse-energy and dijet-mass resolution, requiring hadron calorimeters with a large hermetic geometric coverage and with fine lateral segmentation.

The design of CMS, detailed in the next section, meets these requirements. The main distinguishing features of CMS are a high-field solenoid, a full-silicon-based inner tracking system, and a homogeneous scintillating-crystals-based electromagnetic calorimeter.

The coordinate system adopted by CMS has the origin centered at the nominal collision point inside the experiment, the y-axis pointing vertically upward, and the x-axis pointing radially inward toward the center of the LHC. Thus, the z-axis points along the beam direction toward the Jura mountains from LHC Point 5. The azimuthal angle ϕ is measured from the x-axis in the x-y plane and the radial coordinate in this plane is denoted by r. The polar angle θ is measured from the z-axis. Pseudorapidity is defined as $\eta = -\ln\tan(\theta/2)$. Thus, the momentum and energy transverse to the beam direction, denoted by p_T and E_T, respectively, are computed from the x and y components. The imbalance of energy measured in the transverse plane is denoted by E_T^{miss}.

1.1 General concept

An important aspect driving the detector design and layout is the choice of the magnetic field configuration for the measurement of the momentum of muons. Large bending power is needed

2008 JINST 3 S08004

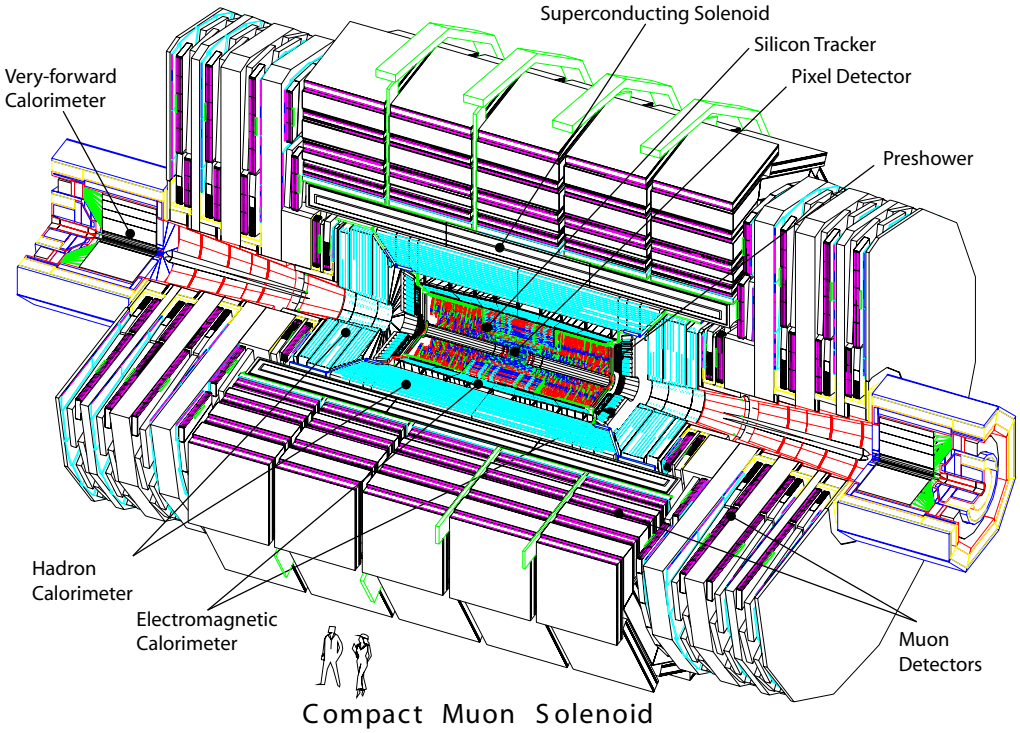

Figure 1.1: A perspective view of the CMS detector.

to measure precisely the momentum of high-energy charged particles. This forces a choice of superconducting technology for the magnets.

The overall layout of CMS [1] is shown in figure 1.1. At the heart of CMS sits a 13-m-long, 6-m-inner-diameter, 4-T superconducting solenoid providing a large bending power (12 Tm) before the muon bending angle is measured by the muon system. The return field is large enough to saturate 1.5 m of iron, allowing 4 muon *stations* to be integrated to ensure robustness and full geometric coverage. Each muon station consists of several layers of aluminium drift tubes (DT) in the barrel region and cathode strip chambers (CSC) in the endcap region, complemented by resistive plate chambers (RPC).

The bore of the magnet coil is large enough to accommodate the inner tracker and the calorimetry inside. The tracking volume is given by a cylinder of 5.8-m length and 2.6-m diameter. In order to deal with high track multiplicities, CMS employs 10 layers of silicon microstrip detectors, which provide the required granularity and precision. In addition, 3 layers of silicon pixel detectors are placed close to the interaction region to improve the measurement of the impact parameter of charged-particle tracks, as well as the position of secondary vertices. The expected muon momentum resolution using only the muon system, using only the inner tracker, and using both sub-detectors is shown in figure 1.2.

The electromagnetic calorimeter (ECAL) uses lead tungstate ($PbWO_4$) crystals with coverage in pseudorapidity up to $|\eta| < 3.0$. The scintillation light is detected by silicon avalanche photodiodes (APDs) in the barrel region and vacuum phototriodes (VPTs) in the endcap region. A preshower system is installed in front of the endcap ECAL for π^0 rejection. The energy resolution

2008 JINST 3 S08004

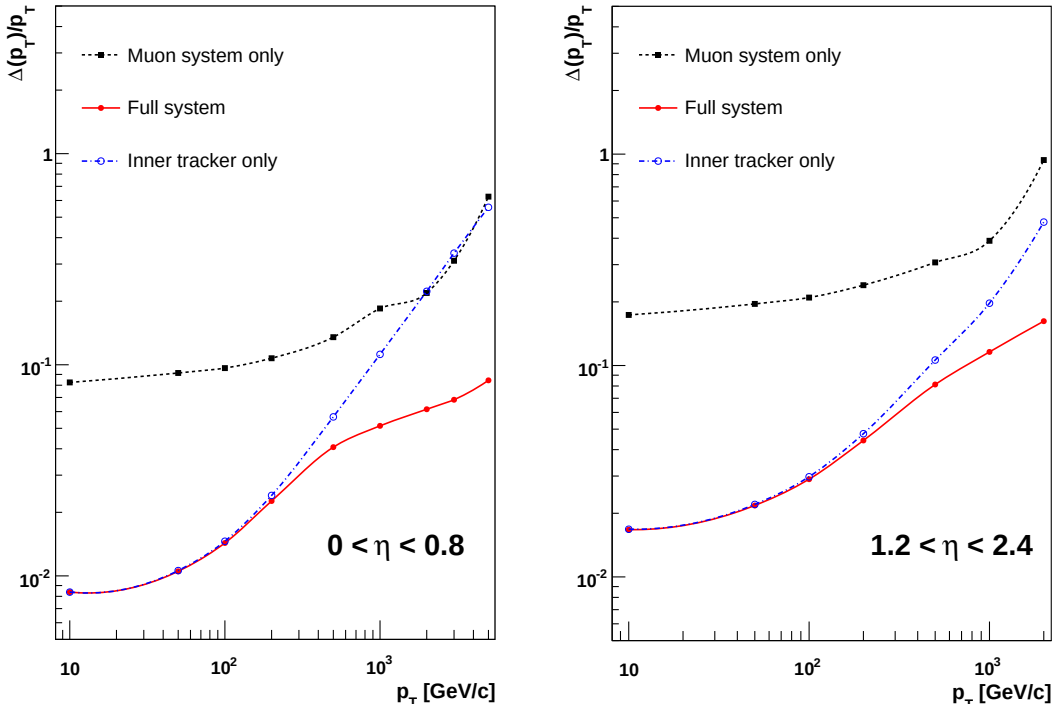

Figure 1.2: The muon transverse-momentum resolution as a function of the transverse-momentum (p_T) using the muon system only, the inner tracking only, and both. Left panel: $|\eta| < 0.8$, right panel: $1.2 < |\eta| < 2.4$.

of the ECAL, for incident electrons as measured in a beam test, is shown in figure 1.3; the stochastic (S), noise (N), and constant (C) terms given in the figure are determined by fitting the measured points to the function

$$\left(\frac{\sigma}{E}\right)^2 = \left(\frac{S}{\sqrt{E}}\right)^2 + \left(\frac{N}{E}\right)^2 + C^2 . \tag{1.1}$$

The ECAL is surrounded by a brass/scintillator sampling hadron calorimeter (HCAL) with coverage up to $|\eta| < 3.0$. The scintillation light is converted by wavelength-shifting (WLS) fibres embedded in the scintillator tiles and channeled to photodetectors via clear fibres. This light is detected by photodetectors (hybrid photodiodes, or HPDs) that can provide gain and operate in high axial magnetic fields. This central calorimetry is complemented by a *tail-catcher* in the barrel region (HO) ensuring that hadronic showers are sampled with nearly 11 hadronic interaction lengths. Coverage up to a pseudorapidity of 5.0 is provided by an iron/quartz-fibre calorimeter. The Cerenkov light emitted in the quartz fibres is detected by photomultipliers. The forward calorimeters ensure full geometric coverage for the measurement of the transverse energy in the event. An even higher forward coverage is obtained with additional dedicated calorimeters (CASTOR, ZDC, not shown in figure 1.1) and with the TOTEM [2] tracking detectors. The expected jet transverse-energy resolution in various pseudorapidity regions is shown in figure 1.4.

The CMS detector is 21.6-m long and has a diameter of 14.6 m. It has a total weight of 12 500 t. The ECAL thickness, in radiation lengths, is larger than 25 X_0, while the HCAL thickness, in interaction lengths, varies in the range 7–11 λ_I (10–15 λ_I with the HO included), depending on η.

2008 JINST 3 S08004

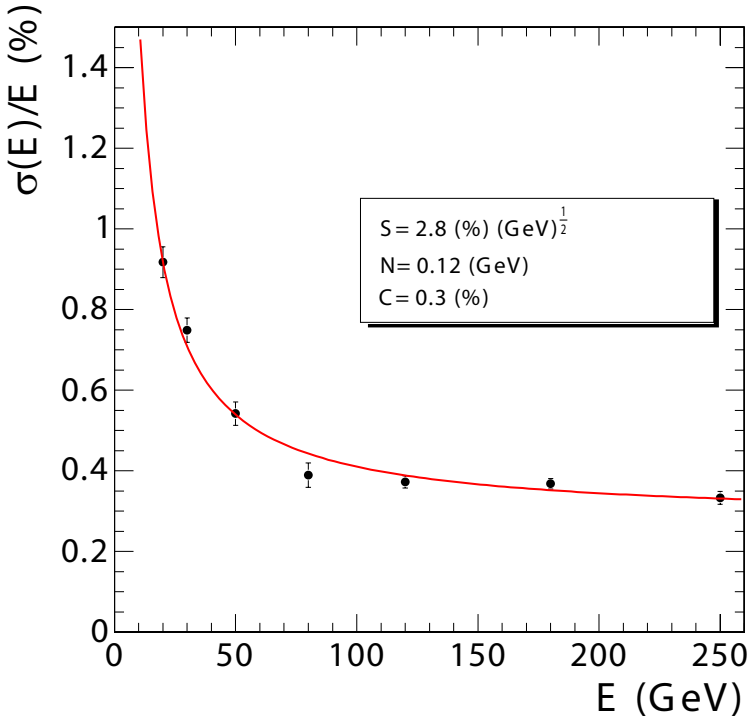

Figure 1.3: ECAL energy resolution, $\sigma(\mathrm{E})/\mathrm{E}$, as a function of electron energy as measured from a beam test. The energy was measured in an array of 3×3 crystals with an electron impacting the central crystal. The points correspond to events taken restricting the incident beam to a narrow (4×4 mm^2) region. The stochastic (S), noise (N), and constant (C) terms are given.

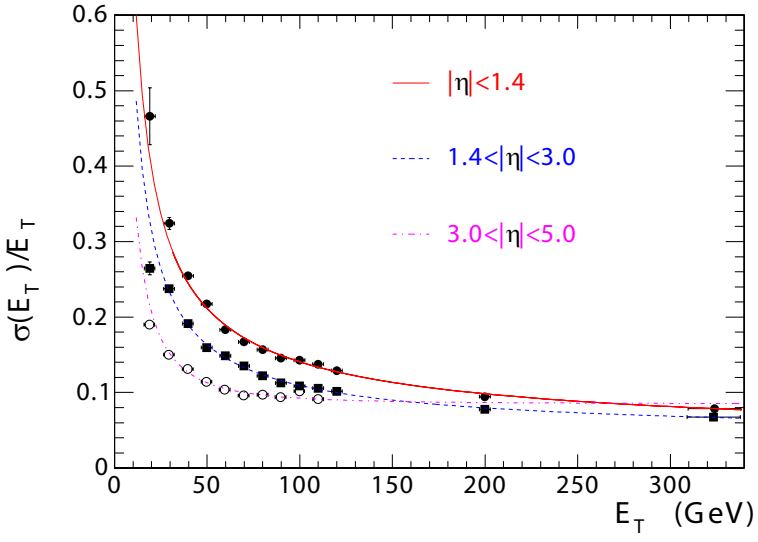

Figure 1.4: The jet transverse-energy resolution as a function of the jet transverse energy for barrel jets ($|\eta| < 1.4$), endcap jets ($1.4 < |\eta| < 3.0$), and very forward jets ($3.0 < |\eta| < 5.0$). The jets are reconstructed with an iterative cone algorithm (cone radius = 0.5).

2008 JINST 3 S08004